J Mater Sci (2008) 43:3435–3440
DOI 10.1007/s10853-007-2336-9

NANOSMAT 2007 - INTERNATIONAL CONFERENCE ON SURFACES, COATINGS AND NANOSTRUCTURED MATERIALS

Boundary-lubricated friction in presence of a nano-well

R. Capozza · A. Fasolino · A. Vanossi ·
M. Ferrario

Received: 31 July 2007 / Accepted: 19 November 2007 / Published online: 6 March 2008

Abstract The advantage of surface macro- and microscopic patterning has been recently proved for improving tribological performances of mechanical sliding contacts. The effects of scaling down the texturing dimensions to the nanoscale have not yet been investigated to a comparable extent. By means of classical Molecular Dynamics simulations, we show that the frictional behavior of a thin film in boundary-lubricated regime is significantly affected by the presence of nanoscale superficial patterning of the moving confining walls, leading to a significant suppression of the high dissipative stick-slip dynamics and a consequent friction reduction. We believe these findings to be relevant for nanotechnology applications.

Introduction

Introduction of specific *micro* textures on sliding surfaces, involving flat and smooth regions interrupted by local depressions, has turned out to be an efficient approach to improve tribological properties of mechanical and technological devices. One recognized effectiveness is that of trapping wear particles. The elimination of wear debris from the matting interface reduces the ploughing component of friction. Another important role of the surface local depressions is to act as reservoir for lubricants capable of feeding it directly between the two contacting surfaces [1, 2].

When a confined lubricant is characterized by a large surface-to-volume ratio, the surface properties strongly affect its tribological properties. In Ref. [3], it is shown how, in presence of patterned surfaces, the concerted effect of wetting properties and surface roughness may considerably reduce friction of a fluid lubricant past the boundaries. Under a certain pressure P_N the micro-scopic patterning reduces the wettability of the substrate, which is only weakly coupled to the liquid lubricant: momentum transfer parallel to the interface is strongly reduced.

If the width of the lubricant is reduced to a few atomic layers, e.g., because of the squeezing of the lubricant out of the contact region due to high load during starting and stopping of interface sliding, the atoms or molecules in the lubricant film are ordered into layers parallel to the bounding walls. Both numerical simulations [4] and experiments [5] generally conclude that the film behaves like a solid (at least in the mechanical sense that static friction is observed) even at temperatures significantly higher than its bulk melting temperature. At low driving relative velocity of the confining walls, the motion in such a system corresponds to the high dissipative stick-slip regime, where a melting-freezing mechanism [4] is observed; the film melts during slip and solidifies at stick.

In this article we investigate the effects of nanoscale surface patterning on the tribological performances of sliding contacts under boundary-lubricated conditions. The meso-scopic frictional response (of the driven wall) is analyzed in terms of the detailed micro-scopic dynamics and structural transitions of the confined lubricant layers under shear.

R. Capozza (✉) · A. Vanossi · M. Ferrario
CNR-INFM National Research Center S3 and Department
of Physics, University of Modena and Reggio Emilia,
Via Campi 213/A, Modena 41100, Italy
e-mail: rcapozza@unimo.it

A. Fasolino
Solid State Theory, Institute for Molecules and Materials,
Radboud University of Nijmegen, Toernooiveld 1,
Nijmegen 6525 ED, The Netherland

From an experimental view point, nanoscale patterns can be suitably created by means of laser surface texturing or by focused ion beam milling.

Recent studies (e.g., the first two cited references) have undoubtedly proved the usefulness of micro-scopic surface patterning for the improvement of mechanical performances of sliding contacts. The effects of scaling down the texturing dimensions to the nanoscale have not yet been investigated to a comparable extent. This is exactly the aim of our theoretical/computational work. A more detailed discussion on experimental surface patterning techniques and applications goes beyond the scopes of our manuscript.

Model

We are interested in the regime of boundary lubrication, when the sliding surfaces are separated by only a few layers of lubricant atoms or molecules. This investigation has at present been restricted to a two-dimensional system consisting of a rigid, patterned substrate (mimicking the texturing of experimental substrates), a moving rigid flat surface (mimicking the driven top wall) and n_l lubricant particles sandwiched in between. Even if quite general cases has been considered, our simulation results mainly focus here on the boundary regime where the lubricant forms three embedded layers. Increasing the film width (always remaining in the boundary-lubricated regime), it has been observed [6] that static friction decreases approximately exponentially. In order to account for possible dependence on wetting and contact angle properties, our 2D modeling will properly deserve future extension to three-dimensional simulations.

The driven top plate and the bottom substrate, characterized here by the same lattice constant $a_s = 1$, are made up of n_t and n_b particles, respectively. We use dimensionless units with top, bottom, and lubricant atoms all having mass $m = 1$. The rigid top substrate of mass $M_{\text{top}} = m\, n_t$ is pulled through a spring, of elastic constant K, connected to a stage which moves along the horizontal x direction with constant velocity V_{ext}. A loading force L is applied to the top plate along the vertical y direction. Due to the vertical confinement, periodic boundary conditions are applied only along the x direction. Considering a non-polar lubricant, all atoms interact via a standard 6–12 Lennard–Jones pairwise potential

$$V_{\alpha\alpha'}(r) = V_{\alpha\alpha'}\left[\left(\frac{r_{\alpha\alpha'}}{r}\right)^{12} - 2\left(\frac{r_{\alpha\alpha'}}{r}\right)^{6}\right] \tag{1}$$

where $\alpha,\alpha' = $ l,t,b refer to lubricant, top and bottom particles, respectively. To reduce the number of parameters, we study the tribological response of the system in the perfect commensurate case where $r_{ll} = r_{tl} = r_{bl}$ ($\equiv r_0 = 1$), focusing on pairwise potentials having the same interaction strength, $V_{ll} = V_{tl} = V_{bl}$ ($\equiv V_0 = 1$). This case may correspond to an intermediate physical situation between that of a "soft" and a "hard" lubricant [7]. The cut-off radius for interactions is $r^* = 2.5\, r_0$. No direct interaction between the top plate and bottom substrate is taken into account. The model is sketched in Fig. 1.

The top plate dynamics satisfies the equations

$$M\ddot{X}_{\text{top}} + \sum_{i=1}^{n_l}\sum_{j=1}^{n_t}\frac{d}{dx_{jt}}V_{t,l}\left(\left|r_{il} - r_{jt}\right|\right) + K\left(X_{\text{top}} - V_{\text{ext}}t\right) = 0,$$
$$M\ddot{Y}_{\text{top}} + \sum_{i=1}^{n_l}\sum_{j=1}^{n_t}\frac{d}{dy_{jt}}V_{t,l}\left(\left|r_{il} - r_{jt}\right|\right) + L = 0, \tag{2}$$

where X_{top} and Y_{top} stand for its center of mass coordinates. The equations of motion for the displacement vectors $\boldsymbol{r}_{il}$ of the n_l lubricant atoms are given by

$$m\ddot{u}_i + \frac{d}{du_i}\sum_{i\neq j}^{n_l} V_{1,1}\left(\left|r_{i1} - r_{j1}\right|\right) + \sum_{\beta=\text{t,b}}\frac{d}{du_i}\left[\sum_{i}^{n_l}\sum_{j}^{n_\beta} V_{\beta,1}\left(\left|r_{i1} - r_{j\beta}\right|\right)\right] + \text{N.H.C.} = 0, \tag{3}$$

where $u_i = x_{il}$ or y_{il}. The temperature control of the system is achieved by means of a Nose'-Hoover chain of thermostats (NHC) acting on the lubricant particles. The coupled equations of motion (2–3) are integrated using the standard fourth-order Runge–Kutta algorithm.

All units are expressed in LJ units V_0, r_0 and the masses of the individual atoms m_0. Taking as an example the interaction parameters between two Xe atoms: $V_0 = 19.83$ meV, $r_0 = 4.055$ Å and $m_0 = 2.16 \times 10^{-22}$ g, e.g., the time unit becomes

$$t_0 = \left(m_0 r_0^2 / V_0\right)^{1/2} = 3.345\,\text{ps}$$

The shape of the pattern groove in the bottom substrate is modeled by means of the Peyrard and Remoissenet potential [8]

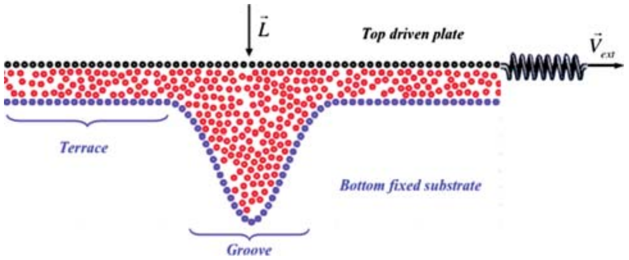

Fig. 1 Sketch of the system. The lubricant is confined between the top driven plate and the patterned substrate. Here the horizontal dimension of the system is 60 (L-J units)

$$V_{\text{sub}}(x) = A\frac{(1+s)^2(1-\cos x)}{1+s^2-2s\cos x}, |s|<1, \tag{4}$$

which has proven to be an efficient on-site potential for describing many realistic situations. The parameter s characterizes the shape of the groove, ranging from spiky narrow dimple to flat large pattern; the parameter A varies the depth. While in the present paper we focus on a fixed choice of the parameter ($s = 0.1$), future investigations will be devoted to a detailed study of the influence of the groove shape on sliding friction.

At the beginning of the simulation procedure, the groove is empty and the particles, confined between top plate and bottom substrate, are ordered in layers and placed at a uniform separation. Due to the applied load L, the lubricant particles start to fill up the available empty space. After a transient time interval Δt_1, the groove turns out to be almost completely filled, and the oscillations of the top plate decrease considerably. Figure 1 shows a typical spatial configuration of the lubricant particles after this system relaxation. Then, the stage attached to the top plate via the spring K starts moving at the constant velocity V_{ext}. A time interval Δt_2 is necessary to reach a steady state dynamics where the bottom groove is filled and three fully discernible layers form between the top plate and the bottom terraces. It is important to note that the number of lubricant particles has been carefully chosen in such a way that the groove fills up and a three layer film is formed with particles uniformly distributed and no intrinsic defects: n_{l} has been actually taken as the largest number for which the film thickness (between the top plate and the bottom terraces) remains equal to three full layers, the addition of extra particles resulting in an unstable situation with thickness irregularly oscillating between three and four layers. At this point, we start calculating and recording the system characteristics of relevant physical interest. In our system the external spring elongation (X_{top} (t)–V_{ext} t) gives a direct measure of the *friction force* experienced by the system. The average friction (*av_fric*)

$$av\_fric = K_{\text{ext}}\langle X_{\text{top}}(t) - V_{\text{ext}}t\rangle \tag{5}$$

is evaluated as the *friction force* averaged over a long enough time interval during the steady sliding state of the system.

In this work we focus on the case of commensurability among the three inherent system "lengths" r_{ll}, r_{tl}, r_{bl}. Experimentally, commensurability is not a common situation and can only be achieved under well-controlled operating conditions [9]. However our situation could represent the physical situation in which, two lubricant layers stick to the confining substrate walls and become "rigid": our rigid substrates would be the lubricant layer stuck on a second rigid (and not necessarily commensurate) substrate. Commensurability means optimal structural match between the crystalline lubricant and the wall. This feature enhances the ordering tendency, which also results from entropy reduction of the disordered molecules near the walls [10]. In our case this increased ordering tendency competes with the disorder effect due to the presence of grooves.

Results

We checked the system response varying two main parameters: the loading force L, and the temperature T. This required to perform a large number of runs with a small time step suitable for atomistic calculations and consequently long simulation times. We found that for a large range of parameters there was a drastic reduction of friction.

However the patterning strongly reduces the friction only when the lubricant does not behave 'liquid-like'. In Fig. 2 a threshold T_{thr} (=0.7) appears: looking at the lubricant *'radial distribution function'* for temperatures above T_{thr}, it turns out that the lubricant is liquid-like and the patterning does not affect significantly the tribological behavior of the system. In this boundary-lubrication regime, viscosity is not supposed to affect much the tribological properties, where the direct interaction between the solid confining surfaces and the lubrication molecules is the crucial factor [4]. While for temperatures under T_{thr} the system is in the so-called high dissipative stick-slip regime: the patterning strongly reduces *av_fric*. The trend of av_fric clearly shows a threshold L_thr (=40) (Fig. 3) also as a function of the external applied load, where we

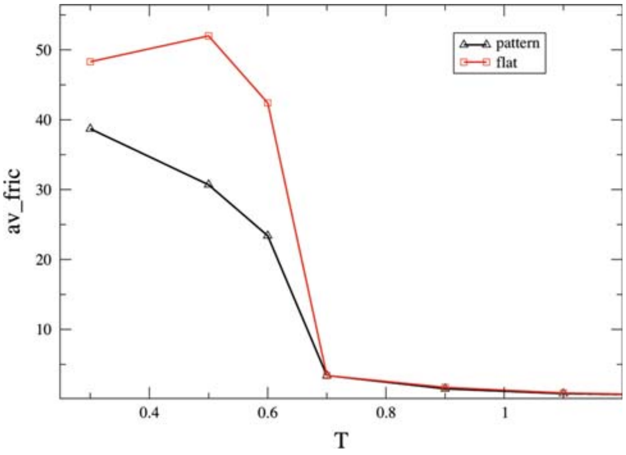

Fig. 2 Average friction as a function of temperature in the case of a flat (*squares*) and a patterned (*triangles*) substrate. There is a sensible reduction of the average friction only under the threshold temperature $T = 0.7$. For higher temperatures, the lubricant is liquid. Here $L = 60$, $V_{\text{ext}} = 0.1$ (L-J units)

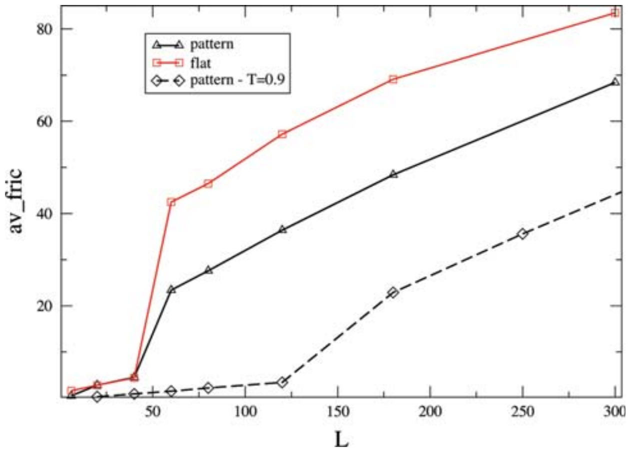

Fig. 3 Average friction as a function of load in the case of a flat (*squares*) and a patterned (*triangles*) substrate. There is a sensible reduction of the average friction above the threshold $L = 40$. For lower loads, the lubricant is liquid. Here $T = 0.6$, $V_{\text{ext}} = 0.1$ (L-J units). The dashed line is (as before) the average friction versus L in the patterned case, but at $T = 0.9$

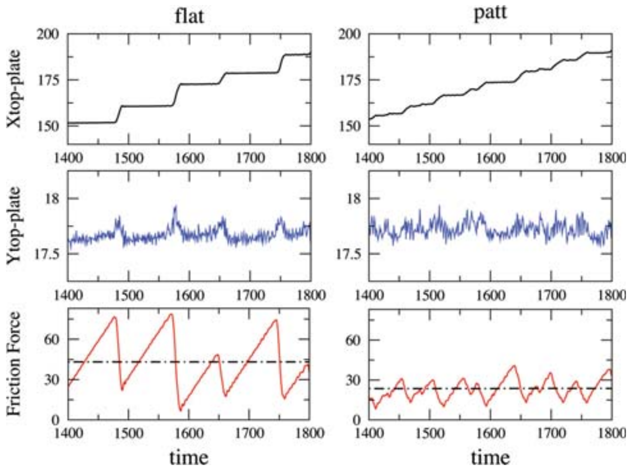

Fig. 4 Comparison between the stick-slip behavior in the case of flat substrate (*left panels*) and patterned substrate (*right panels*). The dashed line represents *av_fric* (average friction). Here $nl = 290$ and 180, in the patterned and the flat case, $T = 0.6$, $k = 7$, $V_{\text{ext}} = 0.1$ (L-J units)

find a liquid-like behavior and smooth sliding for loads lower than L_thr, while a stick-slip regime is observed above L_thr; in the latter case, the pressure is sufficient to induce a solid-like phase in the lubricant due to the vertical confinement. Fixing a higher value of temperature, and plotting *av_fric* as a function of the applied load, we only see (as we could expect) an increase of the threshold load (Fig. 3).

In the case of boundary-lubricating regime, we have observed the occurrence of the stick-slip dynamics for a large range of external driving velocities: the faster is the stage velocity, the smaller is the stick-slip period. In order to investigate the effectiveness of the surface patterning, in terms of friction reduction, on high dissipative sliding regimes, we focused on the behavior of the system for such a velocity V_{ext} that the stick-slip is not suppressed and its time periodicity is sufficiently short. In this way the *friction force* can be correctly averaged on the time interval accessible by the simulation.

Besides in a large range of parameters, for suitable applied loads and temperatures, there is a drastic reduction of friction as shown in Fig. 4. The curves represent the values of the x and y coordinates of the top plate and the *friction force* as a function of time in the flat and patterned case. The x coordinate of the top plate clearly shows a step-like behavior: in the stick phase (flat regions) the external work is accumulated in potential energy of the spring while in the slip phase this energy is converted in kinetic energy of the moving top plate.

In correspondence of each 'slip', the top plate goes up (y coordinate) and quickly comes down (in order to overcame the potential barrier due to the geometrical interlocking between the rigid top plate and the solid lubricant). The main effect of patterning is the mitigation of the stick-slip regime with a consequent reduction of friction.

Now we want to understand which is the state of the lubricant in the "*reduced-friction*" regime (for suitable applied L, T, and V_{ext}). The answer is not easy because our system shows an alternation of a static (stick) and dynamical (slip) phase. Then we must distinguish between the stick and slip phase. In the flat case the g(r) calculation shows a clear peaks structure in the stick phase (characteristic of an hexagonal structure), and a more liquid-like structure in the slip phase (Fig. 5b). This is not surprising and is related to the well-known stick-slip melting-freezing mechanism often reported in literature [4]. Moreover, in the case of a patterned substrate, we never find a solid-like structure neither in the stick nor in the slip phase (Fig. 5a): the difference between the stick and slip phase is not so evident. We can only state that the lubricant is more ordered in the stick phase with respect to the slip phase.

In literature the confinement-induced liquid–solid transitions are well known. By reducing the distance between two confining flat walls to few atomic lubricant layers it is possible to induce a layering and often a solidification: the confinement decreases the entropy of the film and shifts the bulk melting transition to higher temperatures and lower pressure. In our system we could expect a solid phase nearby the terraces and a liquid one in the groove, where the lubricant particles are far apart from the substrates. In Ref. [10] a system of molecules confined between two smooth walls is studied by means of a mean-field theory for confinement-induced phase transition, based on a Ginzburg-Landau expression for the free energy. They show the existence of a *surface-ordered* phase in presence of a

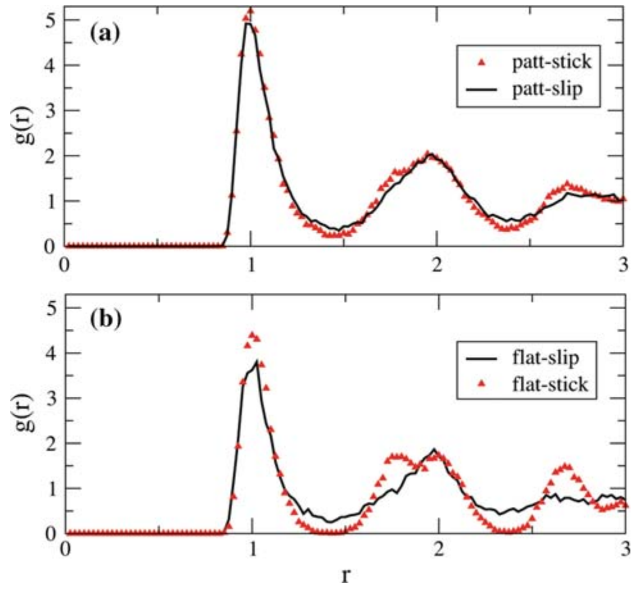

Fig. 5 Radial distribution function calculation g(r) (**a**) *g(r)* calculation in the case of patterned substrate in the stick (*red triangles*) and slip (*solid line*) phase. (**b**) *g(r)* calculation in the case of a flat substrate in the stick (*red triangles*) and slip (*solid line*) phase. In the stick phase the peaks are the typical one of an hexagonal structure

“*large enough reduction of the surface free energy achieved by surface ordering*”. In this case the phase diagram includes an additional region in which the layers adjacent to the walls are crystalline but at the center the ordering almost vanishes. In our case we think that structural match, due to the perfect commensurability between the solid lubricant lattice constant and the one of substrate, enhances the surface ordering tendency. So our system could stay in the *surface-ordered* phase, which is not a fully crystalline phase. The little diffusive tendency, also visible in the flat case (Fig. 6), supports this hypothesis. But this is not surprising: some experimental studies [11] also conclude that the confinement-induced “solidification” does not consist of a well-definite crystallized structure. The patterning destroys the horizontal ordering generated by the flat walls and induces a melting nearby the grooves. Figure 6 reports the trajectories of all lubricant particles in a time interval $\Delta t = 200$ in the flat case and in the patterned case.

The figures show how the lubricant dynamics is influenced by patterning also where the particles are far from the grooves: the diffusion between the three ordered lubricant layers is strongly enhanced, also in correspondence of the terraces (points between layers). This increase is especially visible on the left of the groove. The diffusion zone is slightly shifted in the opposite direction with respect to the direction of motion of the top (right).

Conclusions and perspectives

The above considerations and results demonstrate that the frictional behavior of a thin lubricant film in boundary-lubricated regime is significantly affected by the presence of nanoscale superficial patterning of the moving confining walls. The main effect of the nano-patterning is the ‘mitigation’ of the high dissipative stick-slip regime and a consequent friction reduction. This mitigation is due to a local melting of the lubricant in correspondence of the grooves and to an increase of the diffusion between the lubricant layers. All our simulation results refer to the same groove geometry (*width = 20, depth = 14 L-J units*).

Some simulations were also devoted to the study of *av_fric* as a function of the groove depth: we kept the

Fig. 6 Trajectories of all lubricant particles for a time interval $\Delta t = 200$. (Top) Flat substrate. (Down) Patterned substrate. The destruction of the hexagonal structure at the center of the groove is clearly visible. The points between layers indicate that the particles pass from a layer to another: the diffusion is increased, especially on the left of the pattern. Here $T = 0.6$, $V_{\mathrm{ext}} = 0.1$, $L = 60$ (L-J units)

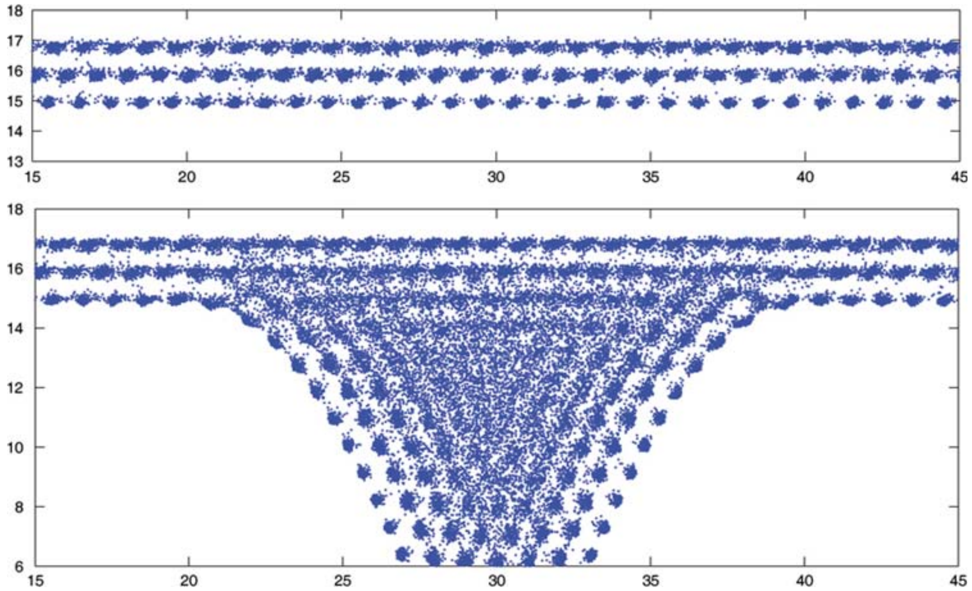

groove *width* constant and varied the *depth.* Some preliminary results show that there is always a threshold depth: grooves deeper than this threshold do not affect further the tribological response of the lubricant.

Future simulations will be also devoted to the study of *av_fric* as a function of the density of the grooves, keeping the shape of the grooves fixed and varying the distance between them. Moreover the stick-slip mechanism is typically dependent on the external velocity: the increase of the sliding velocity leads to a disappearance of the stick-slip. We will study *av_fric* as a function of the external dragging velocity in terms of the detailed micro-scopic dynamics and structural transitions of the confined lubricant.

Acknowledgements This work was supported by: The HPC-EUROPA project (R113-CT-2003-506079), with the support of the European Community—Research Infrastructure Action under the FP6 "Structuring the European Research Area" Programme. PRRIITT (Regione Emilia Romagna), Net-Lab "Surfaces & Coatings for Advanced Mechanics and Nanomechanics" (SUP&RMAN).

References

1. Pettersson U, Jacobson S (2004) Tribol Lett 17:553
2. Blatter A, Maillat M, Pimenov SM, Shafeevc GA, Simakin AV (1998) Tribol Lett 4:237
3. Cottin-Bizonne C, Barrat JL, Bocquet L, Charlaix E (2003) Nat Mater 2:237
4. Persson BNJ (1999) In: Sliding friction: physical principles and applications. Springer-Verlag, Berlin, 1998; Surf Sci Reports 33:83
5. Klein J, Kumacheva E (1998) J Chem Phys 108 (16):6996
6. Braun OM, Peyrard M (2001) Phys Rev E 63:046110
7. Braun OM, Peyrard M (2003) Phys Rev E 68:011506
8. Peyrard M, Remoissenet M (1982) Phys Rev B 26:2886
9. Smith ED, Robbins MO, Cieplak M (1996) Phys Rev B 54:8252
10. Weinstein A, Safran SA (1998) Europhys Lett 42:61
11. Mukhopadhyay A, Zhao J, Bae SC, Granick S (2002) Phys Lett 89:136103